Grading effects in semiconductor nanowires with longitudinal heterostructures

Andrey Chaves,* J. A. K. Freire,† and G. A. Farias‡
Departamento de Física, Universidade Federal do Ceará, Caixa Postal 6030, Campus do Pici, 60455-900 Fortaleza, Ceará, Brazil
(Received 16 June 2008; revised manuscript received 8 September 2008; published 6 October 2008)

The role of graded interfaces between materials in a cylindrical free-standing quantum wire with longitudinal heterostructures is theoretically investigated by solving the Schrödinger equation within the effective-mass approximation. Previous works on such wires with abrupt interfaces have predicted that, as the wire radius is reduced, the effective potential along the growth direction is altered and might lead to a carrier confinement at the barriers, as in a type-II system. Our results show that when graded interfaces are considered, such potential acquires a peculiar form, which presents cusps at the interfacial regions yielding to electron confinement at interfaces. Numerical results also show that, in some special cases, interfacial confinement and type-I to type-II transitions can also be induced by applying a magnetic field parallel to the wire axis.

DOI: 10.1103/PhysRevB.78.155306 PACS number(s): 73.21.Hb, 73.43.Cd

I. INTRODUCTION

Semiconductor nanowires have attracted much interest due to their electronic and optical properties owing to their one dimensionality and possible quantum confinement effects in two dimensions.[1] In the past few years, many research groups have reported the growth of semiconductor nanowires with longitudinal heterostructures, namely, superlattice nanowires (SLNW).[2,3] Much theoretical and experimental study has been made about such wires, where potential applications of these structures as nanobar codes, waveguides, light-emitting diodes, and lasers have been suggested.[4–6]

Lin and Dresselhaus[7] have theoretically investigated SLNW composed by PbS, PbSe, and PbTe, and it was shown that they are promising systems for thermoelectric applications. A hybrid pulse laser ablation/chemical vapor deposition (PLA-CVD) process was developed by Wu *et al.*[8] for the synthesis of single-crystalline nanowires with periodic longitudinal Si/SiGe heterostructures. Moreover, it was suggested that these nanowires could be used as important building blocks for constructing nanoscale electronic circuits and devices. The fabrication of high quality InP/InAs SLNW by chemical beam epitaxy has been reported by Samuelson and co-workers,[2,9] where it reached a high degree of control of size and electron number of such systems. A recent publication by Gudiksen *et al.*[4] has presented high-resolution transmission electron microscopy (TEM) images and composition analysis of a GaAs/GaP SLNW, synthesized by laser-assisted catalytic growth. It was revealed that the transition between GaAs and GaP layers is not atomically abrupt but rather exhibits a graded interface of 15–20 nm for a ~20 nm diameter Au catalyst. Their results indicate that for a smaller wire radius the interface would be reduced, and a 5-nm-diameter SLNW, e.g., should have variations of <5 nm across the junction interfaces.

Calculations based on the one-band effective-mass theory were made by Lew Yan Voon and Willatzen[10] for studying the electronic states in free-standing (i.e., not embedded in a matrix) GaAs/AlAs and InAs/InP SLNW. They predicted the existence of a barrier localization of longitudinal states, as in a type-II confinement potential,[11] which is induced by the strengthening of the radial confinement for thin wires. Their results indicated the possibility of this modulated structure to display free-carrier-like behavior along the nanowire axis when a critical wire radius is considered. These predictions were confirmed later by Willatzen *et al.*[12] Moreover, it has been shown that the existence of critical radii for inversion of state localization is much more general and it is also present in multiband based calculations.[13] Although some of the experimental work in the literature has demonstrated gradual transitions between the heterostructure materials,[4] all of these theoretical investigations on SLNW have dealt only with models for abrupt interfaces, and the existence of graded interfaces was neglected.

In the present work, the effective-mass approximation is used to describe the confinement of electrons in a cylindrical free-standing quantum wire (QWR) with longitudinal heterostructures under an applied magnetic field parallel to the wire axis. In our model, the existence of graded interfaces between materials is taken into account, and the effective mass is assumed to depend on spatial coordinates.[14] This model has been applied to the description of confined states of GaP/GaAs and InP/InAs QWRs. Numerical results confirm the predictions of previous studies in the literature: indeed, for abrupt interfaces, as the wire radius becomes thinner, a change in longitudinal localization of carriers is induced by the creation of a steplike effective potential, composed by the heterostructure bands mismatch and the radial confinement energy. In this case, a critical radius can also be found where the longitudinal effective potential has a band offset equal to zero, which makes the electron behave like a free carrier along the wire axis, despite the presence of a heterostructure. However, considering smooth interfaces, the effective potentials along the wire axis acquire a peculiar form, in which electron states may be confined inside traps formed at the interfacial regions, even for a small interface thickness (less than 5 nm). This result allows us to discard any possibility of having free-carrier-like behavior in such wires with nonabrupt interfaces. Our model also shows that, for excited states, such features of abrupt and nonabrupt QWR can be observed not only by reducing the wire radius but also by increasing the intensity of a magnetic field parallel to the wire axis. This can be an interesting result for device applications, since it demonstrates that a change in longitudinal

potential and carrier localization in heterostructured free-standing QWR can be obtained just by tuning an external parameter, namely, the magnetic-field intensity.

The paper is organized as follows: in Sec. II, we present our theoretical model for the description of electronic states in heterostructured QWR with graded interfaces under applied magnetic fields. In Sec. III, the results for GaP/GaAs and InP/InAs QWR are presented and discussed. Finally, in Sec. IV, we present our conclusions.

II. THEORETICAL MODEL

Our system consists of a circular cylindrical quantum wire at an infinite potential region with a single longitudinal heterostructure. In cylindrical coordinates, the inclusion of a magnetic-field potential into the Hamiltonian, for a $\vec{B}=B\hat{z}$ field, is made through the symmetric gauge vector potential, namely $\vec{A}=\frac{1}{2}B\rho\hat{\theta}$. Hence, the Schrödinger equation for this system, within the effective-mass approximation, is given by

$$\left\{-\frac{\hbar^2}{2m^{\parallel}(z)}\left[\frac{1}{\rho}\frac{\partial}{\partial\rho}\left(\rho\frac{\partial}{\partial\rho}\right)+\frac{1}{\rho^2}\frac{\partial^2}{\partial\theta^2}\right]-\frac{\hbar^2}{2}\frac{\partial}{\partial z}\frac{1}{m^{\perp}(z)}\frac{\partial}{\partial z}-\frac{i}{2}\hbar\omega_c\frac{\partial}{\partial\theta}+\frac{1}{8}m^{\parallel}\omega_c^2\rho^2+V(\rho,z)\right\}\Psi(\rho,z)=E\Psi(\rho,z), \tag{1}$$

where $\omega_c=eB/m^{\parallel}$ is the cyclotron angular frequency and $m^{\perp}$ ($m^{\parallel}$) is the longitudinal (in-plane) mass, which depends on z, since there is a heterostructure along this axis. For a QWR with a R radius, the potential function is defined as $V(\rho,z)=V^{\text{het}}(z)$ for $\rho\leq R$, and $V(\rho,z)=\infty$ otherwise, where $V^{\text{het}}(z)$ is the heterostructure quantum well potential. For numerical examples, we have used the parameters for GaP/GaAs and InP/InAs heterostructures obtained in Ref. 15. For a better description of the interfacial layer between materials, the existence of graded interfaces is taken into account, considering a $XP_{\chi}As_{1-\chi}$ (X=Ga or In) alloy at this region and assuming that the P composition χ varies linearly with z from one (XP) to zero (XAs). Moreover, it also assumes that $m^{\perp}(z)=m^{\perp}_{XP}\chi(z)+m^{\perp}_{XAs}[1-\chi(z)]$ and $V^{\text{het}}(z)=Q_e[\varepsilon_1\chi(z)+\varepsilon_2\chi^2(z)]$, where ε_1 and ε_2 are interpolation parameters and Q_e is the conduction-band offset.[15] This approach is similar to the model of Oliveira *et al.*[16] but now the in-plane mass is also assumed to depend on the material composition $m^{\parallel}(z)=m^{\parallel}_{XP}\chi(z)+m^{\parallel}_{XAs}[1-\chi(z)]$. It is important to point out that this one-band approach within the effective-mass approximation for heterostructured QWR is good for studying only conduction-band states while the description of valence-band states must be made by a $k\cdot p$ multiband model.[13]

To solve Eq. (1), we start from a separation of variables. The solution in θ is chosen as $(1/\sqrt{2\pi})e^{il\theta}$, where $l=0,\pm1,\pm2,\ldots$ is the angular momentum. This leads to

$$\left[-\frac{\hbar^2}{2m^{\parallel}(z)}\frac{1}{\rho}\frac{\partial}{\partial\rho}\left(\rho\frac{\partial}{\partial\rho}\right)+\frac{\hbar^2l^2}{2m^{\parallel}(z)\rho^2}+\frac{l}{2}\hbar\omega_c+\frac{1}{8}m^{\parallel}\omega_c^2\rho^2\right]R_{n,l}(\rho)=E^{(\rho)}_{n,l}R_{n,l}(\rho) \tag{2}$$

for the radial confinement. If ρ is transformed as $\xi=\rho^2/2a_c$, where $a_c=(\hbar/eB)^{1/2}$ is the cyclotron radius, Eq. (2) is rewritten as

$$\xi\frac{d^2R(\xi)}{d\xi^2}+\frac{dR(\xi)}{d\xi}-\left(\frac{l}{2}+\frac{l^2}{4\xi}+\frac{\xi}{4}-\frac{E}{\hbar\omega_c}\right)R(\xi)=0. \tag{3}$$

It is reasonable to try a solution of the form $R(\xi)=\xi^{|l|/2}\exp[-\xi/2]F(\xi)$, where the polynomial and asymptotic behaviors of $R(\xi)$ are explicit. With this solution, Eq. (3) becomes

$$\xi\frac{d^2F(\xi)}{d\xi^2}+[(|l|+1)-\xi]\frac{dF(\xi)}{d\xi}-\left(\frac{l}{2}+\frac{|l|}{2}+\frac{1}{2}-\frac{E}{\hbar\omega_c}\right)F(\xi)=0. \tag{4}$$

This equation is easily identified as a confluent hypergeometric equation, namely $xy''+(c-x)y'-ay=0$, which is solved in terms of Kummer functions.[17] The eigenfunctions are then found as

$$R_{n,l}(\rho_i)=N\xi^{|l|/2}\exp[-\xi/2]F(-x_{n,|l|},|l|+1,\xi), \tag{5}$$

where N is the normalizing parameter and $F(\alpha,\beta,\xi)$ is the Kummer function of the first kind, which remains finite at $\xi=0$. From the boundary condition, since $\Psi(R,z_i)=0$, one has $F(-x_{n,|l|},|l|+1,\xi_R)=0$; hence $x_{n,|l|}$ must be the nth zero of $F(-x_{n,|l|},|l|+1,R^2/2a_c)$. The radial confinement energies are given by

$$E^{(\rho)}_{n,l}=\hbar\omega_c\left(x_{n,|l|}+\frac{l}{2}+\frac{|l|}{2}+\frac{1}{2}\right), \tag{6}$$

which clearly depends on z since ω_c depends on $m^{\parallel}(z)$. Then, this energy must be added as a potential in the remaining equation for this coordinate, yielding

$$\left[-\frac{\hbar^2}{2}\frac{\partial}{\partial z}\left(\frac{1}{m^{\perp}(z)}\frac{\partial}{\partial z}\right)+V_{\text{eff}}(z)\right]Z_m(z)=E_{n,l,m}Z_m(z), \tag{7}$$

where $V_{\text{eff}}(z)=V^{\text{het}}(z)+E^{(\rho)}_{n,l}(z)$ for the heterostructure longitudinal confinement, which is solved by a finite differences scheme.

It is straightforward to show that Eq. (2) becomes the Bessel equation when $B\to0$, giving the Bessel functions of the first kind as eigenfunctions, i.e., $R_{n,l}(\rho)=J_l(x_{n,l}\rho/R)$, and then the energies are given by $E^{(\rho)}_{n,l}(z)=\hbar^2x^2_{n,l}/2m^{\parallel}(z)$. Indeed, the former and the latter functions agree with Eqs. (5) and (6), respectively, when the limit of small B is taken.[17]

III. RESULTS AND DISCUSSIONS

We have calculated the electron confinement energies for cylindrical QWR with longitudinal heterostructures with graded interfaces under applied magnetic fields. The material parameters are considered as $m_{\text{GaAs}}=0.063m_0$ ($m_{\text{InAs}}=0.027m_0$) and $m_{\text{GaP}}=0.33m_0$ ($m_{\text{InP}}=0.077m_0$) for electron effective masses, $\varepsilon_1=-1.473$ eV and $\varepsilon_2=0.146$ eV ($\varepsilon_1=-1.083$ eV and $\varepsilon_2=0.091$ eV) for the interpolation parameters, and the conduction-band offset is assumed as $Q_e=0.5$ ($Q_e=0.68$) for GaP/GaAs (InP/InAs) heterostructures.[15]

Figure 1(a) illustrates a representative sketch of our model of heterostructured QWR. The darker regions represent the

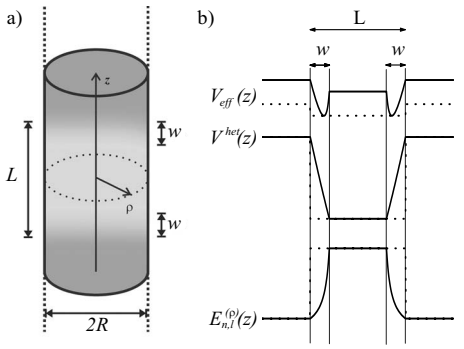

FIG. 1. (a) Sketch of a cylindrical QWR with wire radius R, consisting of a single-quantum well of width L and considering an interface thickness w. (b) Potential profiles along z for abrupt (dotted) and smooth (solid) interfaces. The vertical thin lines denote the limits of the interfacial regions.

material of the barrier, whereas the lighter one represents the material that compounds the well. There is a smooth change from one region to the other, which represents the existence of graded interfaces. In Fig. 1(b), a qualitative scheme shows the potentials $V^{\text{het}}(z)$, due to the bands mismatch between the heterostructure materials, and $E^{(\rho)}_{n,l}(z)$, due to the lateral confinement, both as functions of z. Looking at this scheme, it seems that $V^{\text{het}}(z)$ exhibits linear behavior at the interfaces but actually it is parabolic in z at this region, as described by the quadratic expression given in Sec. II. In fact, with this expression, it can be easily shown that z at the interfacial region is far from the vertex of the parabola describing the potential at the interfaces and, consequently, the quadratic curve in this region looks linear. Since the effective masses at InAs and GaAs are lighter than the ones at InP and GaP, respectively, the lateral confinement energy $E^{(\rho)}_{n,l}$ is higher at GaAs (InAs) than at GaP (InP); hence $E^{(\rho)}_{n,l}(z)$ presents a barrierlike profile because this energy depends on the inverse of the effective mass. Besides, a reduction in the wire radius enhances this barrierlike potential since $E^{(\rho)}_{n,l}$ also depends on the inverse of the squared radius. The effective confinement potential $V_{\text{eff}}(z)=V^{\text{het}}(z)+E^{(\rho)}_{n,l}(z)$ is also illustrated in Fig. 1(b), where one observes that, depending on the wire parameters, it can exhibit a peculiar form where cusps appear at the interfacial regions. The effective potential $V_{\text{eff}}(z)$ is adjusted so that the energy referential is at the GaP (InP) layers.

Figure 2 shows the confinement energies $E_{n,l,m}$ of electrons in the absence of magnetic fields for $E_{1,0,1}$ (symbols) and $E_{1,1,1}$ (curves) states in a GaP/GaAs QWR as a function of the well width L, formed by the longitudinal heterostructure. We have considered interface thicknesses of (a) $w=0$ and (b) 20 Å between materials, and two values for the wire radius R:35 (○, solid) and 75 Å (△, dotted), which are a small and a large value of wire radius, in order to observe the different behaviors due to stronger or weaker bidimensional confinements. The electron wave functions for $l=1$ states in a $L=200$ Å nonabrupt QWR with $R=35$ Å and $R=75$ Å (points marked by arrows) are plotted in Fig. 4(a) for further analysis. For abrupt interfaces, all energies decrease as the well width L is enlarged, as usually observed in quantum wells. However, when graded interfaces are taken into account in a $R=35$ Å wire, the energy of the electron $l=1$ state

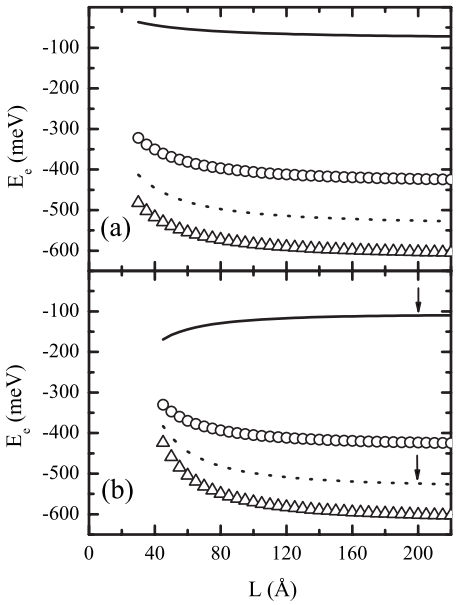

FIG. 2. Electron confinement energies in a cylindrical quantum wire with a longitudinal GaP/GaAs heterostructure with interface thickness (a) 0 and (b) 20 Å, as a function of the well width L for $l=0$ (symbols) and $l=1$ (curves). Two values of the wire radius R were considered: 35 (○, solid) and 75 Å (△, dotted). The electron wave functions for the points indicated by arrows ($L=200$ Å) are plotted in Fig. 4(a).

increases with the well width for small values of L. This indicates that this state is now confined at the interfacial regions so that an enlargement on the well width L further separates the interfaces and increases the confinement energy of the $n=1$ state, analogous to the case of confinement in double quantum wells.[18] On the other hand, $l=0$ states for $R=35$ Å and the states for $R=75$ Å keep the same qualitative behavior for abrupt and $w=20$ Å interfaces, i.e., their energies decrease as increasing L. But quantitatively, the presence of graded interfaces still plays an important role, giving a significative blueshift on these energies specially for small L and large R. As a numerical example, for $L=45$ Å, the energy blueshift due to the graded interfaces, given by $\Delta E_e=E_e(w=20)-E_e(w=0)$, is about $\Delta E_e \simeq 30$ meV (105 meV) for $l=0$ states in a $R=35$ Å (75 Å) QWR. This blueshift, in confinement energies for nonabrupt heterostructures, has also been predicted in quantum wells, *core-shell* QWR, and quantum dots with graded interfaces.[19–21] In fact, for large wire radius, $E^{(\rho)}_{n,l}(z)$ is small; thus the presence of graded interfaces only reduces the confinement region in $V^{\text{het}}_i(z)$, enhancing the energy levels. Yet, for small R, the presence of an interfacial region creates cusps that can confine carriers [see Fig. 1(b), solid], which are responsible for the reduction in the energy blueshift due to interfaces in this case and can even lead to a redshift, as observed for $l=1$ when $R=35$ Å.

As was just discussed, the interfacial confinement for electron lower energy states, as well as the type-I (well) to type-II (barrier) transition in effective potential predicted in previous works,[13] are found for small values of R, which can be troublesome for experimental verification of these fea-

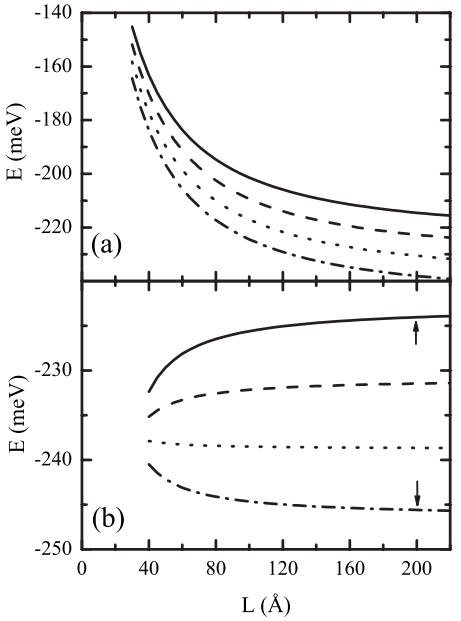

FIG. 3. Electron confinement energies as functions of the well width L for $l=1$ states in a cylindrical GaP/GaAs QWR with wire radius $R=42$ Å, considering (a) abrupt and (b) $w=20$ Å interfaces, under applied magnetic fields $B=0$ (dashed dotted), 10 (dotted), 20 (dashed), and 30 T (solid). The electron wave functions for the points indicated by arrows ($L=200$ Å) are plotted in Fig. 4(b).

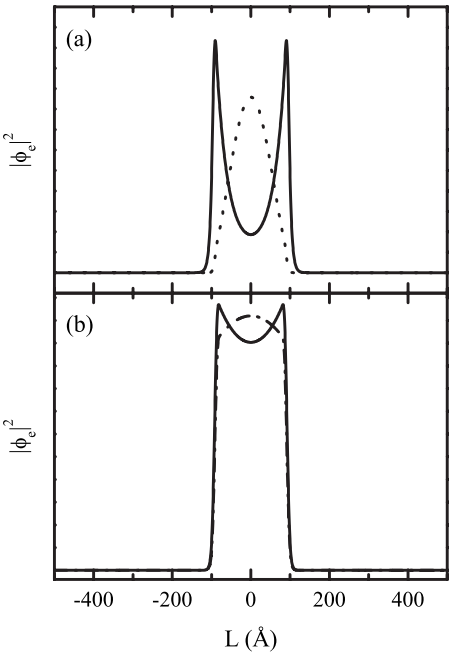

FIG. 4. Electron wave functions for $l=1$ states in a cylindrical GaP/GaAs QWR with graded interfaces of $w=20$ Å thickness and well width $L=200$ Å, as a function of z, considering (a) wire radius $R=35$ (solid) and 75 Å (dotted) in the absence of magnetic fields; and (b) magnetic fields $B=0$ (dashed dotted) and 30 T (solid) for a $R=42$ Å wire radius.

tures of QWR. Nevertheless, one could try to find another way to induce these variations on the carrier´s localization: the main effect produced by reducing the QWR radius is that the carrier´s wave functions are squeezed toward the wire axis. If a magnetic field is applied parallel to the wire axis, the same effect can be obtained; hence, type-I to type-II transitions and interfacial confinements, which were found for wires with small radii, are expected to be found for high magnetic fields as well.

Figure 3 is then devoted to the study of the influence of an applied magnetic field parallel to the wire axis on the confinement energies of electrons. The energies of $l=1$ states in a GaP/GaAs QWR with $R=42$ Å are shown as functions of the well width L, considering (a) $w=0$ Å and (b) $w=20$ Å. Four values of magnetic field are considered: $B=0$ (dashed dotted), 10 (dotted), 20 (dashed), and 30 T (solid). The $l=0$ states are not shown because the dependence of such states on the magnetic field is negligible; $l=1$ states are much more affected by increasing this field since, in the Hamiltonian of Eq. (2), there is an additional term involving the cyclotron frequency ω_c and the angular momentum l. The electron wave functions of $l=1$ states in the nonabrupt case with $L=200$ Å, for $B=0$ and 30 T (points marked by arrows), are plotted in Fig. 4(b) for further analysis. For abrupt interfaces [Fig. 3(a)], the presence of a magnetic field enhances the confinement energies but gives no appreciable change in qualitative behavior of $E_e \times L$ curves. However, considering graded interfaces [Fig. 3(b)], these curves are qualitatively different: the energy behavior for $B=20$ (dashed) and 30 T (solid) is crescent as the well width L increases, whereas the opposite behavior is observed for $B=0$ (dashed dotted) and 10 T (dotted). This can be understood as an interfacial confinement of these states, not induced by reducing the wire radius, as in Fig. 2(b), but due to the presence of a magnetic field parallel to the wire axis. Numerical results obtained from our model demonstrate that, keeping the same interface thickness $w=20$ Å but considering a slightly smaller radius, $R=40$ Å, the electron would be already confined at the interface so that there is no need for applying a magnetic field to observe this kind of confinement. However, with $R=40$ Å and a smaller interface thickness $w=15$ Å, the electron is confined at the GaAs layer. Moreover, in this case, interfacial confinements induced by magnetic fields were also found but only for $B \gtrsim 30$ T, which is higher than the values for $R=42$ Å and $w=20$ Å shown in Fig. 3(b), where a $B=20$ T magnetic field was enough for inducing an interfacial confinement. Our results also predict that interfacial confinement of $l=1$ electrons due to magnetic fields can be found in InP/InAs QWR, as well, with a slightly larger radius $R=48$ Å (not shown in this work). This can be an interesting feature of these systems since, once the QWR has grown, its radius is fixed and an external parameter, namely the magnetic field, can just be tuned to obtain an electron confinement at the well or at the interfaces.

The interfacial confinement of states in GaP/GaAs QWR can be verified by analyzing the electron wave functions as a function of z in such systems, which is illustrated in Fig. 4, for $E_{1,1,1}$ states. In Fig. 4(a), two values of wire radius are considered in the absence of magnetic fields, while in Fig. 4(b) the wire radius is kept and two values of magnetic field are considered. It can be observed in Fig. 4(a) that a confinement of $l=1$ states at the interfaces is induced when the wire radius is reduced from $R=75$ (dotted) to 35 Å (solid). When

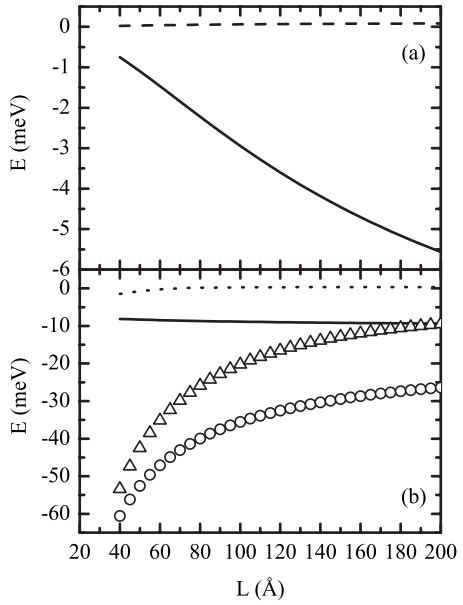

FIG. 5. (a) Electron confinement energies as functions of the well width L for $l=1$ states in a cylindrical InP/InAs QWR with wire radius $R=45$ Å and abrupt interfaces under applied magnetic fields $B=0$ (solid) and 10 T (dashed). (b) The same as (a) but considering graded interfaces of $w=5$ (curves) and 20 Å (symbols), and magnetic fields $B=0$ (solid, ○) and 20 T (dotted, △).

a magnetic field is applied, in Fig. 4(b), the wave function of such states in a $R=42$ Å QWR is also altered, and for $B=30$ T (solid), two peaks at the interfacial regions can be seen. Thus, these results confirm that, in the presence of graded interfaces, confined states at the interfacial regions are observed by reducing the wire radius or increasing the magnetic field intensity.

In Fig. 5, we present the electron confinement energies as a function of the well width L for $l=1$ states in InP/InAs QWR with $R=45$ Å. These results demonstrate that the type-I to type-II transition predicted in previous work on abrupt wires can also be obtained by increasing the intensity of a magnetic field parallel to the wire axis: for $w=0$ Å [Fig. 5(a)], the confinement energies for $B=0$ (solid) decrease with increasing L, but for $B=10$ T (dashed) $E_{1,1,1}=0$ for all L, which shows that these states are not confined in z despite the presence of a heterostructure. This indicates that the radial confinement energy $E_{n,l}^{(\rho)}(z)$ for $B=10$ T, which is a barrierlike potential, is high enough to suppress the contribution of the heterostructure potential in $V_{\text{eff}}(z)$ for this system, yielding a type-II effective potential. Hence, with a InP/InAs QWR with abrupt interfaces, one could control the electron band offset or even change from a confinement to a scattering potential for $l\neq 0$ states just by setting the external magnetic field. However, real QWR are shown to present graded interfaces, and taking them into account in Fig. 5(b), the results show that if one considers an interface thickness $w=20$ Å (symbols), e.g., the magnetic field does not change the qualitative behavior of $l=1$ electrons, which are confined at the interfaces for both $B=0$ (○) and 20 T (△). For a small interface thickness $w=5$ Å (curves), in the absence of magnetic fields (solid), the electron $l=1$ state is confined at the InAs (well) layer and it depends weakly on the well width due to the new form of $V_{\text{eff}}(z)$: for L varying from 40 to 200 Å considering $w=0$ Å, $E_{1,1,1}$ decreases in ~5 meV, whereas for $w=5$ Å, it varies only ~1 meV. For a $B=20$ T magnetic field, considering $w=5$ Å (dotted), a weak interfacial confinement of $l=1$ electrons is still observed for L lower than ~80 Å, while for greater values of L, the barrier on the effective potential is large enough to avoid confinement at the interfaces, leading to $E_{1,1,1}=0$ with an electron localization at the InP layers just like in a type-II system. Thus, for a perfect type-I to type-II transition induced by a magnetic field in InP/InAs nonabrupt QWR, one would need a $R=45$ Å wire with a large InAs layer and small interfaces (<5 Å), i.e., with a very high quality of heterostructure modulation, in order to avoid interfacial confinements.

The presence of magnetic fields has been shown to induce interfacial confinement for $l=1$ states because this field enhances the radial confinement energy $E_{n,l}^{(\rho)}$ and then supports this change of localization. However, for $l=-1$ states, the magnetic field reduces $E_{n,l}^{(\rho)}$; hence, it would never induce a change from well to interfacial localization of such states. Conversely, there are some cases where the $l=-1$ electron state is already confined at the interfaces, for instance, in a GaP/GaAs QWR with $R=39$ Å and $w=15$ Å, and a magnetic field $B=30$ T can induce a transition from interfacial to well localization. Such a transition can also be obtained with $R=40$ Å and $w=20$ but applying a higher magnetic-field intensity, $B=35$ T.

Since the mass variation through the interfacial regions is of major importance for the effective potential and, consequently, for the carriers confinement, it is worthwhile to discuss on the possible types of function which can be used to describe such a variation. In present work, as one can verify in Sec. II, the interfacial region is assumed to be a $X\text{P}_{\chi}\text{As}_{1-\chi}$ (X=Ga or In) alloy with a P composition $\chi(z)$ varying linearly along z at the interfaces. The effective masses are then assumed to depend linearly on $\chi(z)$. However, other dependencies on $\chi(z)$, for instance, a linear dependence for the reciprocal effective mass, i.e., $1/m(z)=(1/m_{X\text{P}})\chi(z)+(1/m_{X\text{As}})[1-\chi(z)]$ could be considered. The following procedure shows straightforwardly that even for this kind of variation one can still tailor the system in order to find confining potentials at the interfaces. Suppose one has a linear function $\chi(z)=z/w$ describing a composition variation at an interface lying within $0\leq z\leq w$, the effective mass and the heterostructure potential are then given by $1/m(z)=A(z/w)+(1/m_{X\text{As}})$ and $V^{\text{het}}(z)=Q_e[\varepsilon_1(z/w)+\varepsilon_2(z/w)^2]$, respectively, with $A=1/m_{X\text{P}}-1/m_{X\text{As}}$. The effective potential in this region is then

$$V_{\text{eff}}(z)=V^{\text{het}}(z)+E_{n,l}^{(\rho)}(z)=a\frac{z}{w}+b\left(\frac{z}{w}\right)^2+C\left(A\frac{z}{w}+\frac{1}{m_{X\text{As}}}\right), \tag{8}$$

where $a=Q_e\varepsilon_1$, $b=Q_e\varepsilon_2$, and C is obtained from Eq. (6) as $C=\hbar eB[x_{n,|l|}+(l/2)+(|l|/2)]$. A minimum value of $V_{\text{eff}}(z)$ exists within $0\leq z\leq w$ if $dV_{\text{eff}}/dz=0$ somewhere in this interval. After some manipulation of the equations, one eventu-

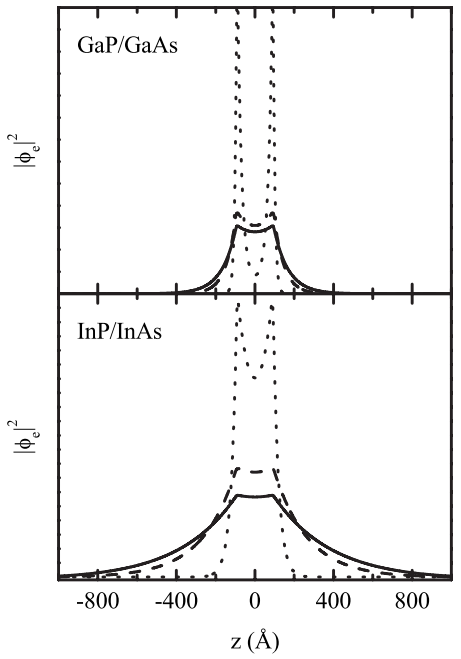

FIG. 6. Electron wave functions for $l=1$ states in cylindrical GaP/GaAs and InP/InAs QWR with graded interfaces of $w=20$ Å thickness and well width $L=200$ Å, as a function of z, considering three different approximations for the effective-mass variation on the interfacial region: direct (dotted) and reciprocal (solid) mass variations considering $\chi(z)$ as an error function, and a variation on the reciprocal mass with a linear function for $\chi(z)$ (dashed). The wire radius is $R=33$ Å ($R=45$ Å) for GaP/GaAs (InP/InAs).

ally finds that a minimum value of $V_{\text{eff}}(z)$ can still occur at the interface for this kind of mass variation, provided $|(CA+a)/(2b)|<1$. The parameters A, a, and b are constants of the material while C is a function of the wire radius R that can be tuned so that this inequality is satisfied. This inequality would be satisfied by no value of C only if $b=0$, i.e., $\varepsilon_2=0$, and this means that the energy gap of the alloy depends linearly on the composition χ, which is not true for most of the materials in the literature.[15] Figure 6 shows the electron wave functions along z for $l=1$ states in GaP/GaAs and InP/InAs QWRs with well width $L=200$ Å and interfaces thickness $w=20$ Å. Dashed line is obtained by considering $\chi(z)$ as a linear function of z and a variation on the reciprocal effective mass $1/m$, whereas the other curves depict the results considering $\chi(z)$ as an error function[5] of z with variations on the direct m (dotted) and reciprocal $1/m$ (solid) effective masses. Electron confinement at interfaces is observed in all the curves shown although for the reciprocal mass cases the electron is just weakly bound in this region and is more dependent on the wire parameters: when the reciprocal mass varies in GaP/GaAs (InP/InAs), the interfacial confinement was found only for $R\sim 33$ Å (~ 45 Å), whereas for a variation in the direct mass used in our model to obtain the previous results of this paper, an interfacial localization is observed for radii varying within a range from $R\sim 27$ to ~ 40 Å ($R\sim 42$ to ~ 46 Å).

The theoretical model we suggest in this work is good for the description of electron states in conduction band. But it fails when studying valence-band states because in cases where the wire diameter $2R$ and the heterostructure width L have almost the same dimensions, the lowest valence state is a combination of heavy-hole (HH) and light-hole (LH) states. Hence, to correctly solve the QWR problem for holes when $2R\simeq L$, one must use a 4×4 Hamiltonian, taking into account HH and LH states. Even so, based on the fact that the changes in localization are strongly dependent on the differences between effective masses, it can be inferred that the critical radii for type-I to type-II transitions, as well as those for interfacial confinements, are not expected to be the same for electrons and holes since the effective masses of these carriers are completely different in each material. Indeed, in a previous work, Lew Yan Voon *et al.*[13] have used a four-band $k\cdot p$ based theory to predict type-I to type-II transitions also for valence-band states in abrupt InGaAs/InP and GaAs/AlAs QWRs, and they found that critical radii are different for electrons and holes. Furthermore, considering a GaAs/GaP QWR, changes in valence-band state localization would hardly be obtained due to the small difference between the hole effective masses in GaAs and GaP. However, changes in the electron localization are found in this system [see Fig. 2(b)]. These electron-hole separations might decrease the overlap between their ground-state wave functions, which would reduce the probability of an interband transition for such states, a feature that is also commonly found in type-II systems.[10] Thus, a low probability of interband transitions would be observed in cases where the hole remains at the well layer and the electron is confined at the interfaces or vice versa.

IV. CONCLUSIONS

The confinement energies of electrons in cylindrical nanowires with longitudinal GaP/GaAs and InP/InAs heterostructures, under an applied magnetic field parallel to the wire axis, were calculated for several values of wire radius, well width, interfaces thickness, and magnetic-field intensity. The difference between effective masses of the heterostructure materials plays an important role in the carrier confinement along the wire axis; it is responsible for creating a z-dependent potential since the lateral confinement energy depends on such masses. It was demonstrated that, for abrupt interfaces, reducing the wire radius leads to a weaker effective confinement potential along the wire axis due to an enhancement of the radial confinement energy. The energies of $l=1$ states are lower than the ones for $l=0$ states, which are due to the fact that the former present higher radial confinement energy, and consequently the effective confinement potential along the wire axis is reduced. The existence of smooth interfaces between materials drastically changes the effective potential profile and can yield to a carrier confinement at the interfacial region for thin wires with $w\neq 0$ instead of the free-carrier behavior or the type-I to type-II transitions predicted in previous works on abrupt QWR.[12,13] Several kinds of functions were considered for the description of the effective-mass variation at the interfaces, and our results demonstrate that an interfacial confinement of carriers can be found for all cases shown. The confinement energies are slightly affected by the presence of magnetic fields, par-

ticularly for $l=0$ states. But in some special cases, increasing the magnetic-field intensity also induces a type-II potential in the abrupt case or a carrier confinement at the interfaces when $w \neq 0$. This can be a useful feature of these systems for device applications since it shows that the carrier behavior can be controlled by an external field. Our results also suggest that in some cases of heterostructured QWR, interband transitions may be strongly suppressed due to spatial separation of electrons and holes states. Finally, the features shown in present work allow us to infer that a high control of composition and size parameters is essential to the design and fabrication of heterostructured quantum wire based devices.

ACKNOWLEDGMENTS

This work has received financial support from the Brazilian National Research Council (CNPq), under Contract No. NanoBioEstruturas 555183/2005-0, Fundação Cearense de Apoio ao Desenvolvimento Científico e Tecnológico (Funcap), and Pronex/CNPq/Funcap.

*andrey@fisica.ufc.br
†Deceased.
‡gil@fisica.ufc.br

[1] M. Law, J. Goldberger, and P. Yang, Annu. Rev. Mater. Res. **34**, 83 (2004).
[2] M. T. Björk, B. J. Ohlsson, T. Sass, A. I. Persson, C. Thelander, M. H. Magnusson, K. Deppert, L. R. Wallenberg, and L. Samuelson, Nano Lett. **2**, 87 (2002).
[3] R. Solanki, J. Huo, J. L. Freeouf, and B. Miner, Appl. Phys. Lett. **81**, 3864 (2002).
[4] M. S. Gudiksen, L. J. Lauhon, J. Wang, D. C. Smith, and C. M. Lieber, Nature (London) **415**, 617 (2002).
[5] C. L. N. Oliveira, A. Chaves, E. W. S. Caetano, M. H. Degani, and J. A. K. Freire, Microelectron. J. **36**, 1049 (2005).
[6] D. Li, Y. Wu, R. Fan, P. Yang, and A. Majumdar, Appl. Phys. Lett. **83**, 3186 (2003).
[7] Y.-M. Lin and M. S. Dresselhaus, Phys. Rev. B **68**, 075304 (2003).
[8] Y. Wu, R. Fan, and P. Yang, Nano Lett. **2**, 83 (2002).
[9] A. Fuhrer, L. E. Fröberg, J. N. Pedersen, M. W. Larsson, A. Wacker, M.-E. Pistol, and L. Samuelson, Nano Lett. **7**, 243 (2007).
[10] L. C. Lew Yan Voon and M. Willatzen, J. Appl. Phys. **93**, 9997 (2003).
[11] H. Grüning, P. J. Klar, W. Heimbrodt, S. Nau, B. Kunert, K. Volz, W. Stolz, and G. Weiser, Physica E (Amsterdam) **21**, 666 (2004).
[12] M. Willatzen, R. V. N. Melnik, C. Galeriu, and L. C. Lew Yan Voon, Math. Comput. Simul. **65**, 385 (2004).
[13] L. C. Lew Yan Voon, B. Lassen, R. Melnik, and M. Willatzen, J. Appl. Phys. **96**, 4660 (2004).
[14] E. C. Ferreira, J. A. P. da Costa, and J. A. K. Freire, Physica E (Amsterdam) **17**, 222 (2003).
[15] E. H. Li, Physica E (Amsterdam) **5**, 215 (2000).
[16] C. L. N. Oliveira, J. A. K. Freire, V. N. Freire, and G. A. Farias, Appl. Surf. Sci. **234**, 38 (2004).
[17] S. V. Branis, G. Li, and K. K. Bajaj, Phys. Rev. B **47**, 1316 (1993).
[18] R. Ferreira and G. Bastard, Rep. Prog. Phys. **60**, 345 (1997).
[19] A. Chaves, J. Costa e Silva, J. A. K. Freire, and G. A. Farias, J. Appl. Phys. **101**, 113703 (2007).
[20] J. Costa e Silva, A. Chaves, J. A. K. Freire, V. N. Freire, and G. A. Farias, Phys. Rev. B **74**, 085317 (2006).
[21] E. W. S. Caetano, M. V. Mesquita, V. N. Freire, and G. A. Farias, Physica E (Amsterdam) **17**, 22 (2003).